Supporting Information

Enabling *in vivo* measurements of nanoparticle concentrations with three-dimensional optoacoustic tomography

Dmitri A. Tsyboulski, Anton V. Liopo Richard Su, Sergey A. Ermilov, Sergei M. Bachilo, R. Bruce Weisman, and Alexander A. Oraevsky

1. Concentration measurements of single-walled carbon nanotubes (SWCNTs) in organs of mice.

To illustrate reliability and accuracy of methodology of measuring SWCNT concentrations in organs of mice the following test experiments were performed. Small aliquots of SWCNT stock suspension in Pluronic were added to samples of homogenized mouse liver prepared as described in the main text to obtain test samples with nanotube concentration of 1, 3 and 5 μg/mL. A 1.5 mL portion of a test sample was placed in a 2 mL centrifuge tube and sonicated for 60 min using 10 s on and 5 s off cycles with an output power of 6 – 8 W. An external ice bath prevented sample heating during sonication. After 10 mins, the sonication was paused and the sample's fluorescence and absorption spectra were measured. The overall duration of sonication was 60 min. Similarly, reference SWCNT solution was prepared by adding 200 μL of stock SWCNT suspension in Pluronic with concentration of ~ 0.43 μg/mL to 4 ml of 2% aqueous sodium deoxycholate (SDOC) solution and sonicating in a similar manner as described above to obtain well-dispersed SWCNT samples with a concentration of 20.5 μg/mL. Figure S1 shows the changes in emission spectra of a test liver sample and the reference SWCNT suspension during sonication. At first ultrasonic treatment breaks SWCNTs aggregates present in Pluronic suspension, which is evidenced as an increase in SWCNT emission signal. After ~40 mins of sonication the sample's fluorescence reaches its maximum and no further emission increase is observed. It is known that continuing sonication results in a gradual and slow decrease in SWCNT fluorescence associated with breaking nanotubes into shorter fragments and introduction of structural defects in SWCNT lattice [1-3]. This process, however, is very slow, and is likely to provide similar degree of SWCNT fluorescence quenching in both reference and organ samples.

Homogenized tissue samples are turbid. Following the sonication procedure the samples become optically clear, which is beneficial for optical measurements (Fig.

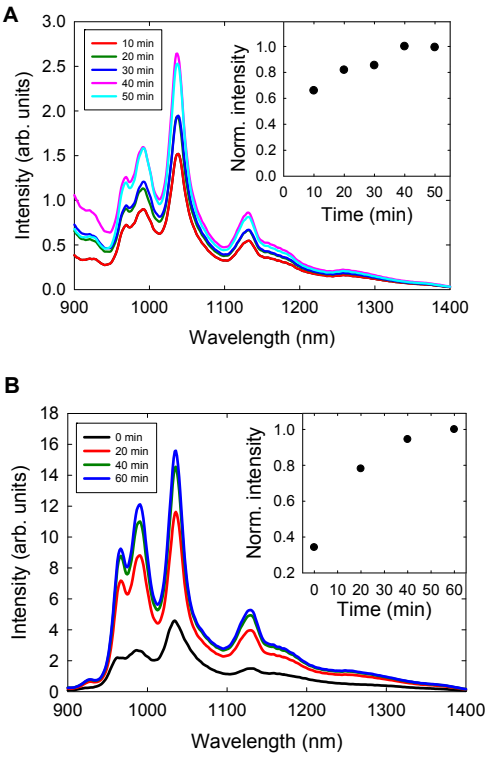

Figure S1. The observed changes in emission spectra of the homogenized liver test sample with SWCNT concentration of 3 μg/mL (a) and reference SWCNT suspension in SDOC (b) during sonication. The inserts show the relative change of SWCNT fluorescence with time.

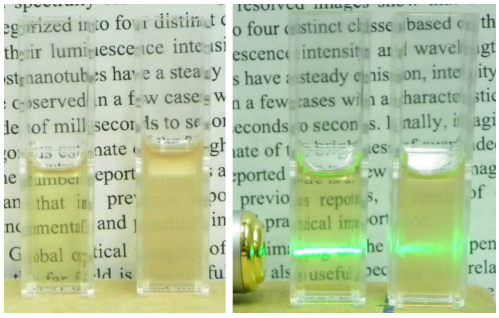

Figure S2. A sample of homogenized liver before (scattering sample) and after sonication (clear sample).

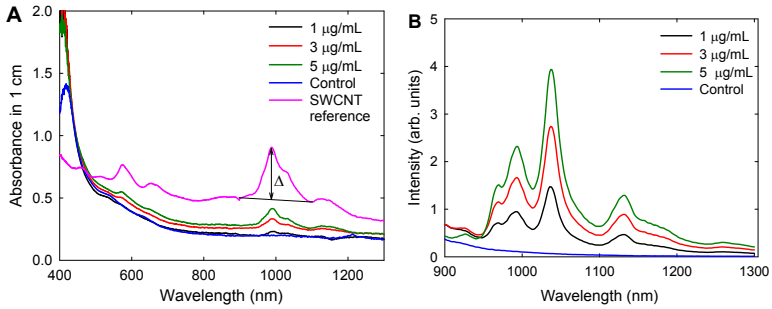

Figure S3. Absorption (a) and emission spectra (b) of test liver samples with SWCNT concentrations of 0, 1, 3 and 5 μg/mL.

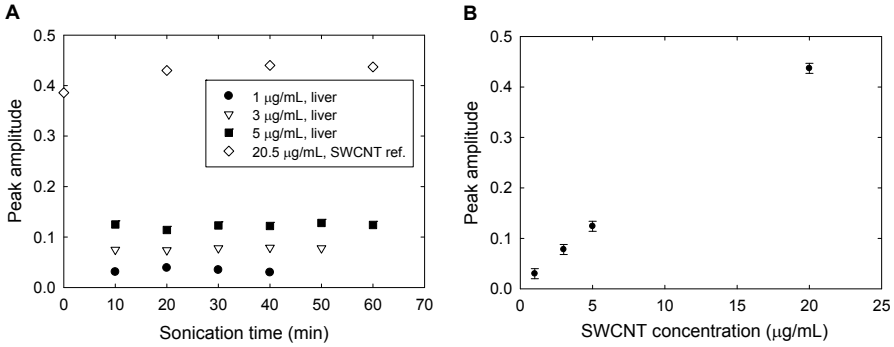

Figure S4. (a) Measured net peak amplitude Δ in test samples of liver as a function of sonication time. (b) The measured net peak amplitude after sonication procedure in the samples from (a).

S2). Figure S3 shows the absorption and emission spectra of processed samples. Small absorption peak at 990 nm is seen in all 3 samples containing nanotubes. As shown at Fig. S4, the net peak amplitude Δ is a stable feature of SWCNT suspensions which does not change noticeably during sonication and therefore can be used to measure SWCNT concentration. Note that measuring nanotube quantities with absorption spectroscopy in biological samples at the level significantly less than 1 μg/mL is difficult. Fluorimetric method allows to measure SWCNT concentrations with much higher sensitivity. It is well known that SWCNT fluorescence is sensitive to a variety of environmental factors, such as pH, salinity, type of surfactants, *etc*. Hence, it is important to account for the influence of SWCNT environment on its emission properties when attempting quantitative measurements. In biological samples, interaction of proteins and their fragments with nanotube coating may potentially affect SWCNT emission efficiency. The presence of such interaction can be detected when comparing spectral profiles of the reference SWCNTs suspension and the test liver samples (Fig. S5). Note that fluorescence of SWCNTs with smaller diameter (emission peaks at 966 and 990 nm) appears slightly quenched as compared to larger diameter nanotubes.

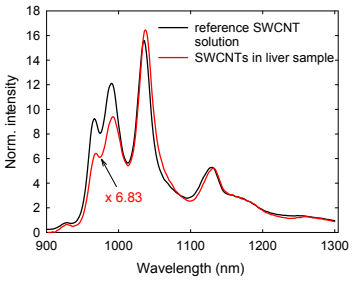

Figure S5. Emission spectra of reference SWCNT suspension and test liver sample with nanotube concentration of 20.5 and 3 μg/mL. Fluorescence background of biological residuals (liver control) was subtracted from the emission spectrum of the liver sample.

To account for these effects, the following procedure is used to measure SWCNT concentrations. After measuring the sample's emission spectrum, the sample is titrated with small volumes of a reference solution with known SWCNT concentration. Measuring

the changes in the sample's emission spectrum allows one to deduce initial SWCNT concentration in a sample. With background emission spectrum of an organ (blue trace, Fig. S3b) and background-corrected emission spectrum of SWCNTs in a sample (red trace, Fig. S5) as basis functions, emission spectra of titrated samples are fitted as a linear combination of basis functions with variable weights using the least square fitting algorithm. SWCNT concentration in the sample then is calculated as:

$$c_0 = \frac{w_0 \cdot \Delta c}{w_1 - w_0} \quad (1),$$

where c_0 is SWCNT concentration in the original sample, Δc is the change in SWCNT concentration after titration, and w_0 and w_1 are the weights of SWCNT components in the original and titrated samples, respectively. Figure S7 illustrates the SWCNT concentration measurement procedure in more detail. SWCNT concentrations in the sample are calculated using eq.1 were 43.3 ± 0.3 μg/ml.

In vivo SWCNTs are exposed to a diverse variety of proteins, enzymes and other compounds present in blood and cells, an environment which can not be modeled *ex vivo*. As a result, emission efficiencies of SWCNTs in real samples may be different. Figure S8 compares the emission spectra of the liver sample from a nanotube-injected mouse and the liver sample with added SWCNTs. Although these spectra appear significantly more similar than those shown at Fig. S5, minor differences can still be observed. While biodistribution studies with transmission electron microscopy have demonstrated that SWCNT framework remains intact and persists in the liver, spleen and other tissues for more than 90 days [4], it remains unknown to what extent and at what rate SWCNT structure can be derivatized or structurally damaged *in vivo*. It is known that nanotube fluorescence quantum yield may be significantly reduced by reactions which remove π-electron from SWCNTs while leaving their structure intact. Excitonic nature of SWCNT fluorescence, and the ability of excitons to diffuse along a nanotube results in exceptionally high sensitivity of SWCNT emission and much lower sensitivity of SWCNT absorption to oxidation or covalent functionalization [5, 6]. If fluorescence efficiency of nanotubes will be reduced *in vivo*, *ex vivo* concentration measurements of SWCNTs based on their absorption and fluorescence signal will show a significant discrepancy. The fact that both of these methods yield nearly the same result (see Fig. 6 in the main text)

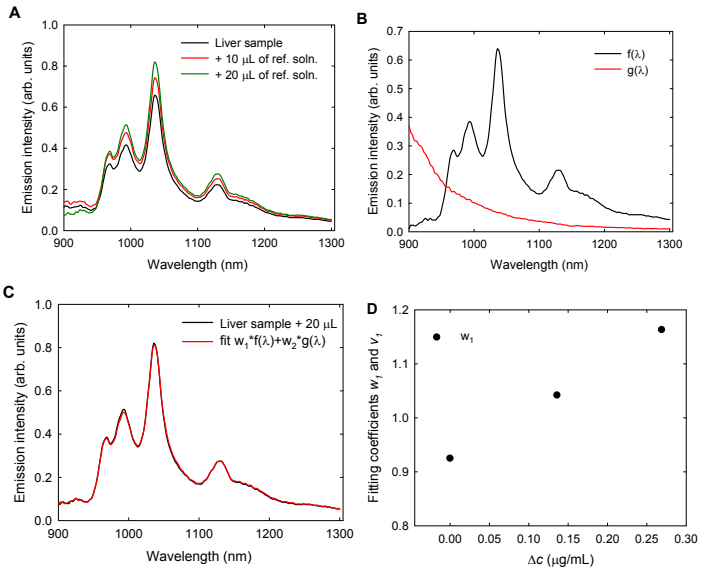

Figure S7. (a) Emission spectrum of a liver sample from nanotube-injected mouse before and after addition of 10 and 20 μL of reference SWCNT solution. (b) Background-corrected emission of SWCNTs in the liver sample f(λ) and fluorescence background of liver control g(λ) used as a basis function in a linear fit. (c) Emission spectrum of the liver sample with added nanotubes and its fit. (d) Weights of f(λ) component of all 3 emission spectra from (a).

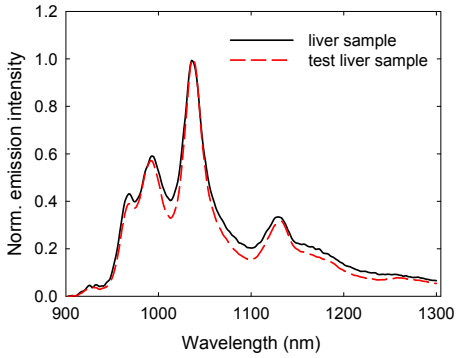

Figure S8. Comparing emission spectra from a liver sample of a nanotube-injected mouse (black line) and a liver sample with added SWCNTs (red).

indicates that absorptivity changes of SWCNT *in vivo* are minor, if present at all, and the estimated changes in organ's μ_a values are correct.

2. On the stability of SWCNT absorption spectra *in vivo*.

In the context of the presented work it is important to assess the magnitude of potential changes in the absorption spectrum of SWCNT ensemble *in vivo*. It is expected that following the injection the initial surfactant coating of SWCNTs will be replaced or modified by biological compounds. Surfactant displacement typically results in a small spectral shift of ~ 1 – 30 nm caused by the change in SWCNT dielectric environment [7-9]. Absorption coefficient of SWCNT stock suspension in Pluornic at the peak maximum which is seen at 997 nm is only ~ 35% higher as compared to μ_a value at the imaging wavelength of 1064 nm (Fig. 2a in the main text). Spectral shift of 20 nm in the first van Hove resonance energies of SWCNTs around 1000 nm (observed in emission spectrum of intravenously injected SWCNTs in Pluronic [9]) will result in 13% increase of μ_a value at 1064 nm. Note that SWCNT emission and thus the magnitude of spectral shift observed is a feature of individualized SWCNT in a suspension. Experiments with density gradient fractionation have conclusively demonstrated that a standard SWCNT suspension procedure employed here yields mostly small crystalline aggregates of several nanotubes and only few percents of truly individualized SWCNTs [1, 10-12]. As a result, absorption spectrum of a whole ensemble appears far less sensitive to changes in SWCNT environment. Figure S9a demonstrates the changes in the absorption spectrum of SWCNTs as they are being suspended in aqueous Pluronic solution. Relatively minor changes in SWCNT absorption spectrum are seen at the imaging wavelength. The absorption spectrum of density-gradient purified SWCNT suspension without small aggregates shown at Fig. S9b is characterized by slightly sharper features. Upon SWCNT aggregation, the spectral broadening will reduce contrast between peak and valleys of the absorption spectrum. However, SWCNT absorption background will not change significantly. Thus, the changes in μ_a value at specific wavelength will remain relatively minor [9, 13].

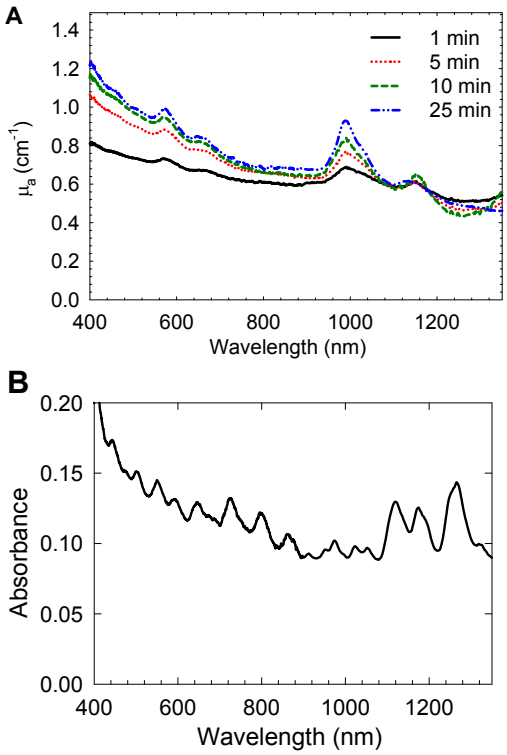

Figure S9. (a) Observed changes in the absorption spectrum of SWCNT suspension in Pluronic during sonication. (b) Absorption spectrum of a density gradient - purified suspension containing only individualized SWCNTs. Note, structural compositions of SWCNTs in (a) and (b) is different.

3. Analysis of nanoparticle aggregation effects on the magnitude of optoacoustic signals.

The magnitude of optoacoustic signals depends on the energy absorbed in a medium and its Gruneisen parameter, which is directly related to the thermal expansion coefficient α of the medium. Non-linear change of α with temperature may result in a non-linear dependence of recorded OA signals on the excitation energy. In heterogeneous media, represented by a suspension of nanoparticles in liquid,

conditions may arise when thermal properties of the localized environment where heating occurs may appear different from those of the bulk volume. The magnitude of optoacoustic signals may depend on the aggregation state of nanoparticles in the suspension. To investigate this potential issue in greater detail we designed an experiment to compare OA signal response from SWCNT samples with markedly different degree of nanoparticle aggregation. The first sample was prepared using density gradient purification technique [12] to obtain SWCNT suspension containing predominantly individual nanotubes. The second SWCNT sample was prepared in a conventional manner, which involved sonicating SWCNT material in an 1% aqueous sodium cholate solution for 20 minutes, followed by a centrifugation at 10,000 g for 20 minutes. The third sample was prepared by sonicating raw SWCNT material in aqueous surfactant solution for 1 min only. From our experience, it is known that if sample #3 were subject to centrifugation in the same manner as sample #2, nearly all SWCNT material would be removed from the suspension. Figure S10 further demonstrates the differences in nanoparticle aggregation state in these samples by comparing their absorption and fluorescence spectra.

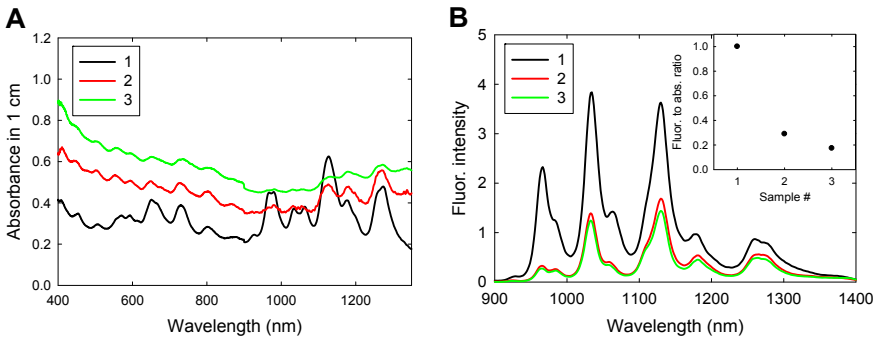

Figure S10. (a) Absorption and (b) fluorescence spectra of SWCNTs samples with different degree of aggregation: 1 – density gradient purified SWCNT sample, containing predominantly individual nanotubes; 2 – SWCNT suspension after 20 min sonication and 20 minutes centrifugation, containing predominantly small SWCNT bundles; 3 – SWCNT suspension after 1 min sonication containing larger SWCNT bundles as compared to sample #2. All SWCNT samples were suspended in 1% aqueous sodium cholate solution. The insert in (b) shows integral fluorescence to integral absorption ratio of recorded spectra.

Absorbance matched suspensions of SWCNTs were prepared for optoacoustic imaging (Fig. S11). Since the sample #1 contained 8.2% of residual iodixanol, additional samples #4 and #5 derived from suspensions #2 and #3, respectively, were prepared by adding iodixanol to the mixtures. Preparing additional samples was necessary given the lack of knowledge about thermal properties of iodixanol/water mixtures. After dilutions, suspension medium in samples 1, 3 and 5 contained 4% iodixanol by weight. Suspensions were sealed in PTFE capillary tubes with 0.64 mm inner diameter and imaged with our OAT system. Figure S11b shows cross-sectional image of these capillaries.

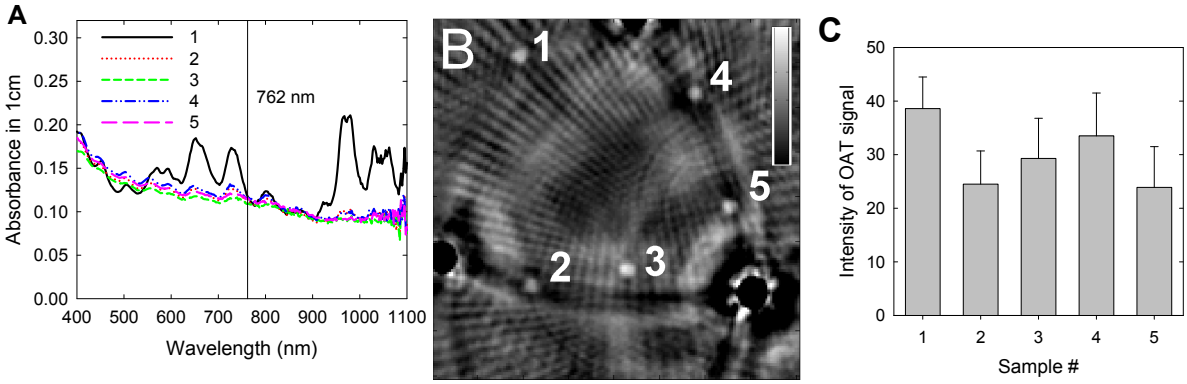

Figure S11. (a) Absorption spectra of SWCNT suspensions used in OAT imaging. Samples have the same absorption at the laser excitation wavelength of 762 nm. (b) Cross-section of an OAT image showing tubes containing SWCNT suspensions 1 – 5. (c) OAT signals from samples 1 – 5 measured from image in B. Peak amplitude was evaluated relative to the average background value in the vicinity of the tube.

There were no significant differences in the magnitude of OA signals from these samples detected in the experiment (Fig. S11c). In a prior study (unpublished work) we have compared OAT signals from absorbance-matched samples of gold nanorods (GNRs) coated polyethylene glycol (PEG), carbon nanotubes suspended in a 2% aqueous sodium cholate, and ~ 3% weight/volume aqueous $NiSO_4$ solution (Fig. S12).

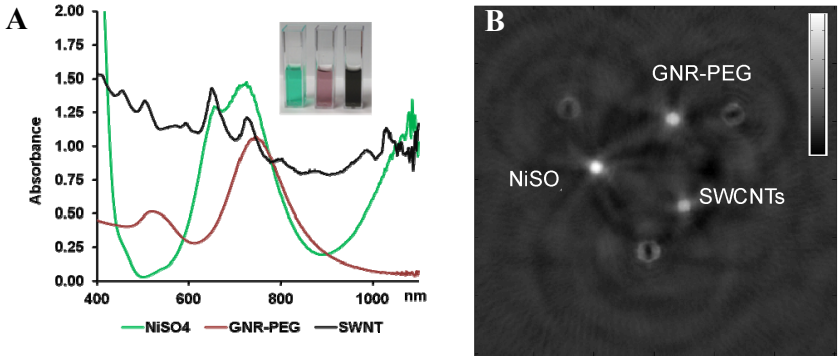

Figure S12. (a) Absorption spectra of test solutions. (b) Cross-section of an OAT image showing tubes containing SWCNTs, GNR-PEG and $NiSO_4$ solutions. The relative values of OA signals from $NiSO_4$, GNR-PEG, and SWCNT samples were 1, 0.73, 0.64, respectively.

While GNRs absorb significantly more energy per particle as compared to SWCNTs, the corresponding OAT signals from GNR-PEG and SWCNT samples were very similar. Note, that SWNCT sample contains 1% surfactant, while GNR-PEG complexes are in pure water, and the presence of surfactant may affect thermal expansion coefficient of the medium. Increased signal from $NiSO_4$ sample is likely caused by the change in α, which is known to increase with water salinity. These observations indicate that the aggregation of SWCNTs *in vivo* will not likely change the magnitude of OA signals significantly.

Reference List

[1] M. J. O'Connell, S. M. Bachilo, C. B. Huffman, V. C. Moore, M. S. Strano, E. H. Haroz, K. L. Rialon, P. J. Boul, W. H. Noon, C. Kittrell, J. P. Ma, R. H. Hauge, R. B. Weisman, and R. E. Smalley, Science **297**, 593-596 (2002).

[2] D. A. Heller, P. W. Barone, and M. S. Strano, Carbon **43**, 651-653 (2005).

[3] A. V. Naumov, D. A. Tsyboulski, S. M. Bachilo, and R. B. Weisman, Chem. Phys. accepted (2013).

[4] S. T. Yang, X. Wang, G. Jia, Y. Gu, T. Wang, H. Nie, C. Ge, H. Wang, and Y. Liu, Toxicol. Lett. **181**, 182-189 (2008).

[5] G. Dukovic, B. E. White, Z. Y. Zhou, F. Wang, S. Jockusch, M. L. Steigerwald, T. F. Heinz, R. A. Friesner, N. J. Turro, and L. E. Brus, J. Am. Chem. Soc. **126**, 15269-15276 (2004).

[6] L. Cognet, D. Tsyboulski, J.-D. R. Rocha, C. D. Doyle, J. M. Tour, and R. B. Weisman, Science **316**, 1465-1468 (2007).

[7] V. C. Moore, M. S. Strano, E. H. Haroz, R. H. Hauge, and R. E. Smalley, Nano Lett. **3**, 1379-1382 (2003).

[8] J. H. Choi, M. S. Strano, Appl. Phys. Lett. **90**, 223114-1-223114-3 (2007).

[9] P. Cherukuri, C. J. Gannon, T. K. Leeuw, H. K. Schmidt, R. E. Smalley, S. A. Curley, and R. B. Weisman, Proc. Natl. Acad. Sci. USA **103**, 18882-18886 (2006).

[10] M. S. Strano, V. C. Moore, M. K. Miller, M. J. Allen, E. H. Haroz, C. Kittrell, R. H. Hauge, and R. E. Smalley, J. Nanosci. Nanotechnol. **3**, 81-86 (2003).

[11] M. S. Arnold, A. A. Green, J. F. Hulvat, S. I. Stupp, and M. C. Hersam, Nat. Nanotechnol. **1**, 60-65 (2006).

[12] S. Gosh, S. M. Bachilo, and R. B. Weisman, Nat. Nanotechnol. **5**, 443-450 (2010).

[13] S. M. Tabakman, K. Welsher, J. S. Hong, and H. J. Dai, J. Phys. Chem. C **114**, 19569-19575 (2010).